

Various properties of OMVPE-grown GaAs epilayers on heavily In-doped substrates

by Tetsuji IMAI*

1. INTRODUCTION

In the previous papers^{1),2),3)}, some detailed experimental studies on the growth behavior of GaAs epitaxial layers prepared in the laboratory with an integrated safety Organo Metallic Vapor Phase Epitaxy (OM-VPE) system have been given. Epitaxially grown GaAs layers on heavily In-doped GaAs substrates exhibited particular phenomena which revealed the occurrence of coherent growth. These phenomena were attributed to the difference in the lattice constant value between the In-doped substrate with the larger value and the undoped GaAs with the smaller one.

In this paper, various properties of OM-VPE grown GaAs epilayers on heavily In-doped GaAs substrates are summarized according to the previous papers^{1),2),3)}.

High-performance gallium arsenide devices such as metal-semiconductor field-effect transistors (MES-FETs), high electron mobility transistors (HEMT), and heterobipolar transistors (HBT) recently show drastic improvements in their performance. They are especially suitable for monolithic microwave integrated circuits (MMIC) and for high-speed digital integrated circuits. These GaAs integrated circuits are mainly prepared in the thin active layers formed on semi-insulating (S. I.) gallium arsenide substrates.

The S. I. gallium arsenide substrates are mainly divided into three different types: namely, Cr-doped, In-doped, and undoped ones. These are usually prepared mainly by the liquid encapsulated Czochralski (LEC) growth method. The formation of the thin active layers on such S. I. substrates is made by molecular beam epitaxy (MBE), OM-VPE, and ion implantation followed by an annealing process. The combination of epitaxial layer formation techniques and the S. I. substrates chosen are different depending on the devices and integrated circuits to be fabricated. The use of OM-VPE on In-doped LEC S. I. substrates is one of the most promising combinations owing to the usage of dislocation-free substrates. Interesting prop-

* 理工学部電気工学科教授 電子情報工学

注) この研究は、静岡大学工学部電子工学科福家俊郎氏との共同研究である。

erties of GaAs epilayers grown on these substrates have been pointed out by Morioka *et al.*⁴⁾. They attributed the origin of these properties to the lattice mismatch between the grown epitaxial layers and the S.I. substrates.

Recently, Shinohara *et al.* reported a series of papers^{5),6),7)} dealing with the generation of misfit dislocations for MBE grown GaAs on In-doped LEC-GaAs substrates. In these papers, they clearly showed that the misfit dislocations were generated at the epilayer / substrate interface owing to the lattice mismatch between the grown GaAs and the heavily In-doped GaAs substrates. It was also clarified that dislocation-free GaAs epilayers could be prepared by In doping of the epilayers grown on the In-doped GaAs substrates. However, in their studies, for the observation of dislocations, the electron-beam-induced current (EBIC) method was employed and therefore, information obtained by these EBIC images mainly gave the microscopic patterns only at the interface region between epilayers and the substrates.

The present paper basically supports the above-mentioned papers and also gives more systematic data about the recovery process from the coherently grown crystalline lattice to that inherent in GaAs. In this case, OM-VPE films were grown primarily on In-doped LEC GaAs substrates and surface morphology was observed by a differential interference microscope. Newly found thermal annealing effects and Zn-doping effects on the lattice constant of the GaAs epilayers grown by OM-VPE on the heavily In-doped GaAs substrates are also reported in this paper.

2. EXPERIMENT

The horizontal reactor OM-VPE apparatus used here was installed inside the experimental laboratory with special regard for safety, due to the extreme toxicity of arsine. This integrated safety OM-VPE apparatus provides a multialarm system as well as a quick air refresh system.

In order to minimize the risk in handling toxic gas in the small scale laboratory, a quick air-refresh system and a sensitive detection and rapid response system were built. A safety system which operates in the event of an emergency has been designed on the basis of the following two considerations. (1) When the toxic gas concentration exceeds the level of the permissible exposure limit, shut-off valves of the toxic gas supply are closed manually and / or automatically in order to minimize the system leak. (2) In the event of contamination by the toxic gas, the forced-air ventilation system is stopped. Thus, the toxic gas concentration in the exhaust to the open air is reduced to below the permissible exposure level (50 ppb) by the installed arsine-adsorption system using FeCl_3 .

Fig. 1 shows the facility layout and the air ventilation system. The toxic gas concentrations in the gas cabinet and in the exhaust to the open air are always monitored. Two independently controlled blowers are provided. Under normal operating conditions, the gas and reactor cabinets, and also the laboratory space, are

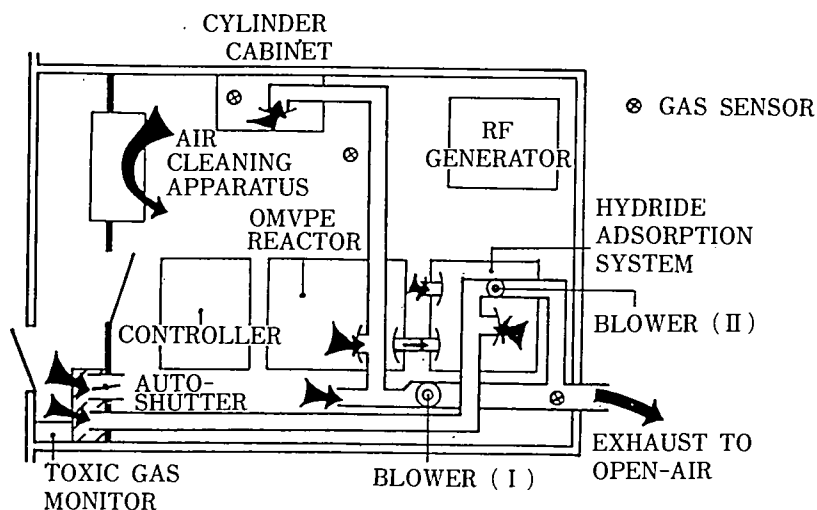


Fig. 1. Layout of an integrated safety OM-VPE system inside the laboratory where gallium-arsenide epitaxial layers are grown.¹⁾

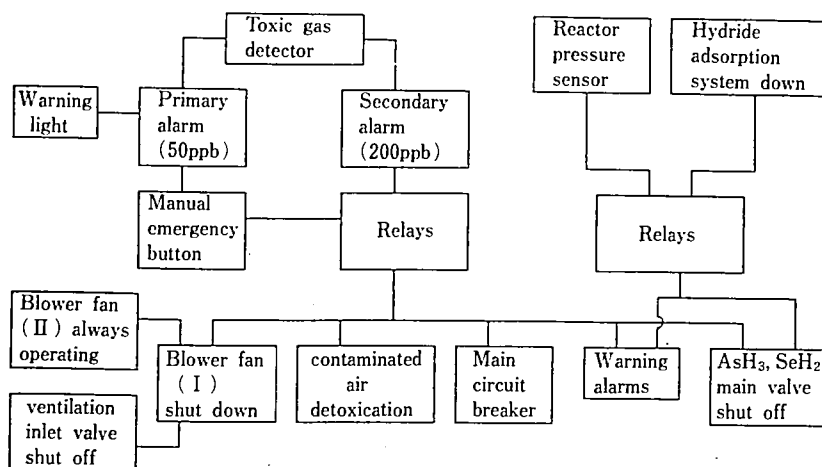


Fig. 2. Outline of the flow chart to maintain safety if the toxic gas sensor detects the two stages of alarm levels. Other emergencies are also automatically controlled to maintain safety.¹⁾

vented at the rate of about $10 \text{ m}^3/\text{min}$ to the open air by blower (I). Blower (II) is used to vent the exhaust from the hydride-adsorption system, diluted by fresh air from outside the laboratory. The air vented to the open air by the two blowers is monitored by the toxic gas sensor. The air in the laboratory is circulated through the air-cleaning apparatus in order to prevent stagnation of the air.

Fig. 2 shows the schematic diagram of an integrated safety system for laboratory

use of a OM-VPE apparatus and the related air refreshing installation. When the toxic gas sensor detects the primary alarm level (50 ppb AsH_3 concentration), the warning light on the indicator panel comes on and the operators push the emergency button using their own judgement. When the secondary alarm (200 ppb AsH_3 concentration) is indicated by the gas sensor, the whole system containing the blower fan (I), except the hydride-adsorption system, is stopped automatically. Hence, if an emergency occurs, the contaminated air is confined in the laboratory and is gradually detoxified by the AsH_3 adsorption system.

If the pressure in the quartz chamber exceeds the predetermined level and the hydride-adsorption system gets beyond the limit of its capability, the epitaxial growth must be terminated. The AsH_3 main valve and the air-operated valves of the gas supply line are then automatically closed.

The mirror-surface GaAs epilayers were obtained at substrate temperatures as low as 500°C with a constant growth rate of $\sim 1.7\mu\text{m/h}$ under the conditions of a V / III ratio of 13.8 and a TMG flow rate of $2.0 \times 10^{-5} \text{ mol / min}$. Throughout this work, the value of the V / III ratio and the TMG flow rate were fixed to these values. The substrate temperature was varied from 500 to 700°C and the growth time was from 15 to 300 min. The substrates used were heavily In-doped (order of $10^{20} / \text{cm}^3$), 0.1-ppm Cr-doped, and undoped LEC-grown (100) GaAs. All of these substrates showed semi-insulating electrical resistivity. As the evaluation methods, differential interference microscopic observation, x-ray analyses, photoluminescence analyses, and etch pit density observation at the epilayer were employed.

3. RESULTS AND DISCUSSIONS

3.1. Surface morphology

Figure 3 shows the surface morphology observed by an differential interference microscope for epilayers grown on undoped substrates. Figures 3 (a) and 3 (b)

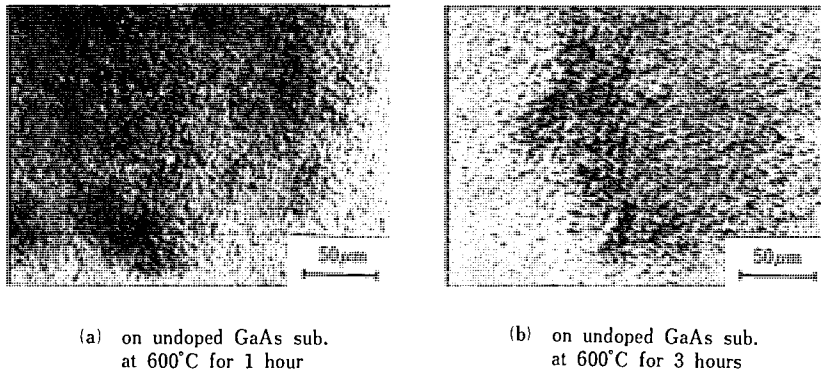


Fig. 3. Differential interference microphotographs of the as-grown surfaces of GaAs epilayers on the undoped GaAs substrates at the substrate temperature of 600°C for (a) 1 and (b) 3 h.²⁾

correspond to specimens obtained at a substrate temperature of 600°C and growth times of 1 and 3 h, respectively. The surface morphology of these specimens was mirror smooth and no significant difference was found between Figs. 3 (a) and 3 (b). The surface morphology for the specimens grown on the Cr-doped substrate showed almost the same patterns as those given in Fig. 3.

In addition, for the undoped and Cr-doped substrates, the surface morphology of epilayers grown at substrate temperatures ranging from 500 to 700°C did not vary either.

Figure 4 shows the surface morphology observed for the epilayers grown on the In-doped substrates. Figures 4 (a) and 4 (b) represent the differential interference microscopic surface patterns obtained for specimens grown at 500°C for 1 and 3 h, respectively. Clear differences are observed between Figs. 4 (a) and 4 (b).

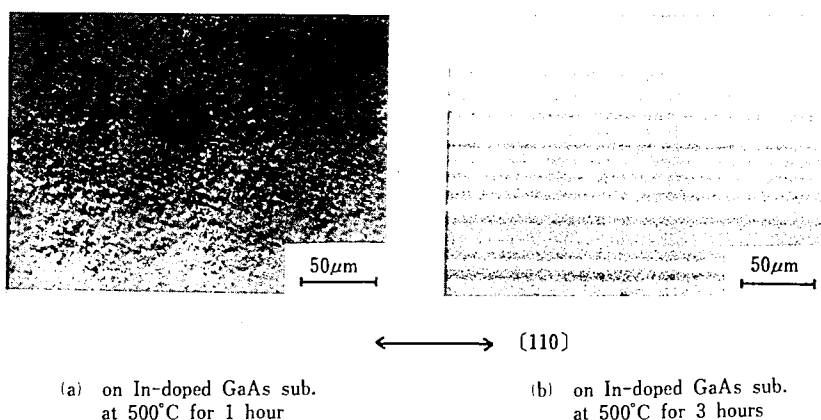


Fig. 4. Differential interference microphotographs of the as-grown surfaces of GaAs epilayers on the In-doped GaAs substrates at the substrate temperature of 500°C for (a) 1 and (b) 3 h.²⁾

Namely, Fig. 4 (a) shows a mirrorlike smooth surface similar to Fig. 3, while Fig. 4 (b) clearly indicates a streaky pattern. The latter is precisely a cross-hatched pattern. Figure 5 shows the surface morphology obtained for the specimens grown at a substrate temperature of 600°C on the In-doped substrates. In this case, even the specimen grown for 1 h shows a streaky pattern roughly similar to that shown in Fig. 4 (b). The specimen grown for 3 h, meanwhile, shows a much smaller separation of streaky lines⁶⁾ compared with the specimen grown for 1 h.

Cross-hatched patterns are known as misfit dislocation arrays generated along the $\langle 110 \rangle$ directions, the $[110]$ and $[1\bar{1}0]$ ones. In this study, surface morphology observations are done by use of differential interference microscope. In such a case, $[110]$ -direction hatching is preferentially observed and $[1\bar{1}0]$ -direction cross-hatched lines are only weakly observed.⁴⁾ If the EBIC method is employed, clear cross-

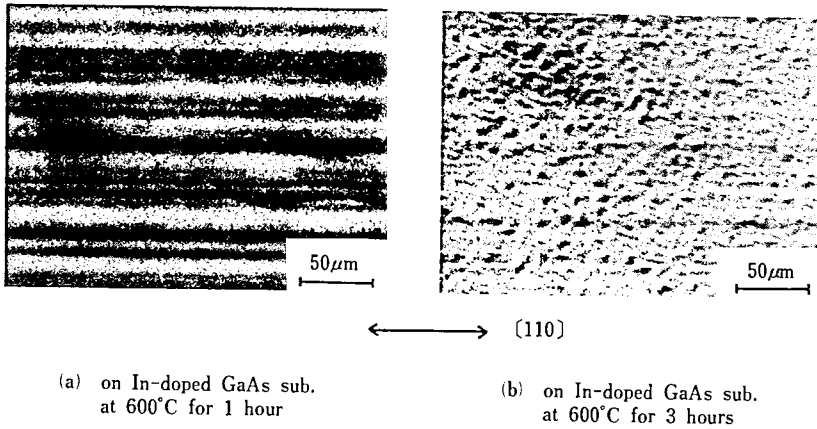


Fig. 5. Differential interference microphotographs of the as-grown surfaces of GaAs epilayers on the In-doped GaAs substrates at the substrate temperature of 600°C for (a) 1 and (b) 3 h.²⁾

hatched patterns (both for $[110]$ and $[1\bar{1}0]$ directions) are observed.^{6),7)}

A summary of the results shown in Figs. 3-5 reveals the following: (1) OM-VPE-grown GaAs layers on both nondoped and Cr-doped S. I. GaAs substrates consist of a crystalline structure with the lattice constant almost the same as that of substrates. Surface morphology of these grown layers is mirrorlike, independent of their growth temperature and growth time within the range examined. (2) The layers grown on heavily In-doped substrates with a larger lattice constant than that inherent in GaAs single crystals indicate various surface morphologies. Furthermore, these are strongly depending on both growth temperature and growth time, or grown epilayer thickness.

3.2 X-ray diffraction analyses

The results mentioned in Sec. 3.1 directly reflect the lattice matching between the epilayers and substrates. This is easily ascertained by x-ray diffraction analyses.^{4),6),1)} Figure 6 indicates x-ray diffraction patterns obtained for three specimens: (a) epilayer on a heavily In-doped GaAs substrate, (b) epilayer on a Cr-doped GaAs substrate, and (c) epilayer on an undoped GaAs substrate. For these three specimens, epitaxial growth time and temperature was 1 h and 600°C, respectively. In the specimen (a), both $K\alpha_1$ and $K\alpha_2$ peaks for (600) crystalline planes split into two peaks, whereas in (b) and (c), the peaks show no splitting. These patterns indicate that the difference of lattice constant between the epilayer and the heavily In-doped GaAs substrate is significant, while no appreciable difference is found between the epilayers on Cr-doped and nondoped GaAs substrates. The values of lattice constants from the results shown in Fig. 6 are 5.6585, 5.6533, and 5.6533 Å with the common error of ± 0.0005 Å for In-doped, Cr-doped, and undoped GaAs substrates,

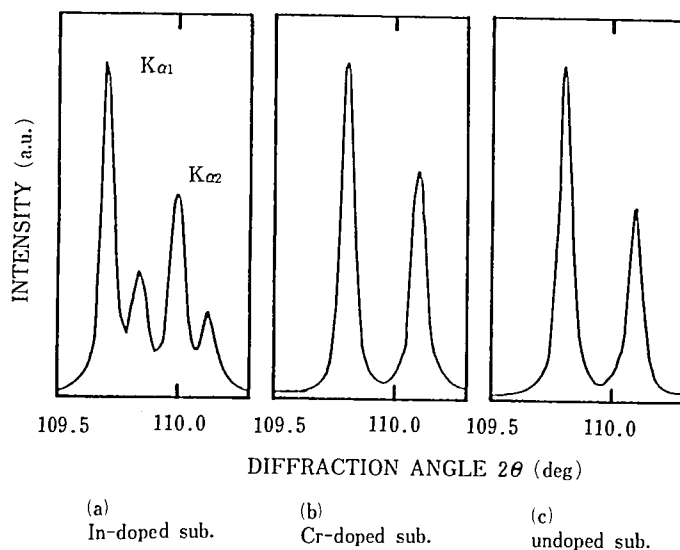


Fig. 6. X-ray diffraction patterns of (600) planes of GaAs epilayers on (a) heavily In-doped GaAs substrate, (b) Cr-doped GaAs substrate, and (c) undoped GaAs substrate.²⁾

respectively.

The values of lattice constants of the epilayers grown on heavily In-doped GaAs substrates are plotted in Fig. 7 versus the epilayer thickness together with the calculated coherently grown lattice constant. The latter is obtained by the formula given by Matthews, Blakeslee, and Mader⁸⁾ and has a value of 5.6486 Å .

3.3. Surface morphology versus lattice constant

The data given in Fig. 7 are obtained for two series of specimens : One is prepared at a substrate temperature of 600°C and the other one is at 500°C . It is obvious that as the layer becomes thicker, the perpendicular lattice constant a_{\perp} becomes larger. This suggests the occurrence of relaxation during the epigrowth process of the crystalline structure, a coherent one to that inherent in pure GaAs. Moreover, it is apparent from Fig. 7 that the series of specimens grown at 500°C make the relaxation occur at a much slower rate than those grown at 600°C , especially for thin layers. Correlating the surface morphology given by Figs. 3-5 with the lattice constant values, it is confirmed that the specimens with lattice constants a_{\perp} larger than about 5.651 Å show the streaky surface morphology. On the other hand, the specimens with values smaller than about 5.651 Å show no structural surface patterns, but merely show mirrorlike surface morphology. This semiquantitative tendency is applicable for both series of specimens, although the growth temperature is different. These aspects are summarized and schematically given by Fig. 8 .

The correspondence between the surface morphology and the lattice constant a_{\perp}

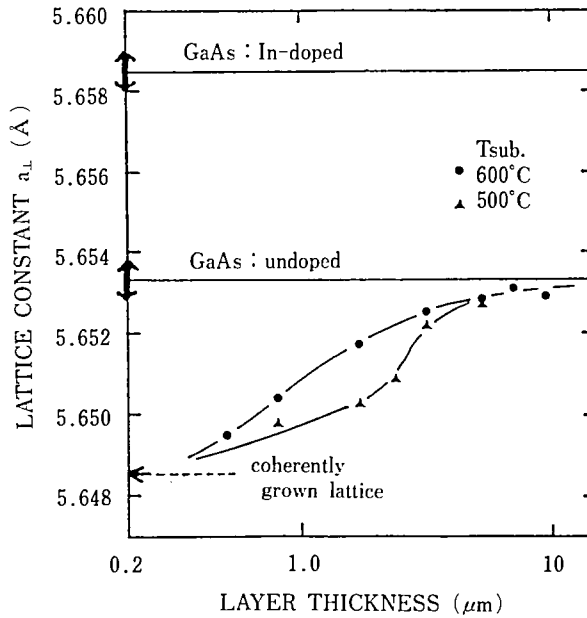


Fig. 7. Lattice constant a_{\perp} perpendicular to the substrate surface against the GaAs epilayer thickness. The substrate temperatures are 500°C (▲) and 600°C (●).²⁾

can be explained as follows: When the layer thickness is thin enough, the coherently grown crystalline lattice is sustained, incorporating the strain caused by the two-dimensionally expanded lattice in the growth plane together with the perpendicularly compressed one. This originates from the heteroepitaxial growth of GaAs on In-doped GaAs with larger lattice constant. As the layer thickness increases, the elastic strain in the grown layers begins to generate dislocations when the accumulated strain due to increasing layer thickness exceeds a critical value. This dislocation generation occurs at the epilayer / substrate interface as a cross-hatched array pattern at first as observed by EBIC.⁶⁾ Then, this propagates toward the surface of the epitaxially grown layers. As a result, crosshatched or rather streaky surface morphology is observed for such specimens. The cross-hatched patterns which initially appear at the epilayer / substrate interface propagate toward the surface, changing its pattern. Namely, the crosshatched dislocation arrays seem to propagate predominantly in the [110] direction selectively during the epigrowth process. Thus, the rather streaky surface morphology is observed. At the same time, this generation of dislocation arrays means the relaxation of elastically expanded lattice, with a resulting increase in the perpendicular lattice constant a_{\perp} .

This is the reason why the correspondence is observed between the epilayer surface morphology and the value of the lattice constant a_{\perp} . For the specimens with

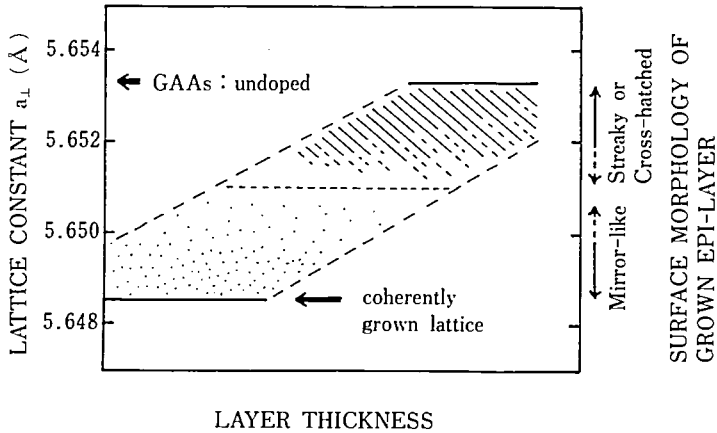


Fig. 8. Schematic diagram showing the correlation between the GaAs epilayer lattice constant a_{\perp} and the surface morphology. Epilayer thickness also strongly correlates both with lattice constant a_{\perp} and the surface morphology.²⁾

smaller values of a_{\perp} only smooth surface morphology is observed, while those with larger values of a_{\perp} indicate streaky or crosshatched surface morphology. The series of specimens grown at lower temperature, 500°C, receive less thermal energy than those grown at higher temperature, 600°C. This explains the difference of lattice-constant (a_{\perp}) increase curves plotted against the layer thickness, in Fig. 7. Higher growth temperature enhances not only the dislocation generation itself but also the propagation of the generated dislocation arrays toward grown layer surfaces.

3.4. Etch-pit density

Etch-pit density (EPD) of the grown layers prepared at 600°C was also measured and the values of EPD were plotted against the layer thickness as shown in Fig. 9. The following is seen from this figure: (1) As the layer thickness increases, the measured EPD increases; (2) when the layer thickness becomes larger than several μm , the values of EPD almost saturate at significantly smaller values than those of the epilayers grown on undoped GaAs substrates.

Comparing the results shown in Figs. 7 and 9, an initially coherent-grown lattice, i. e., dislocation-free lattice, generates dislocations of the order of $(5-12) \times 10^3/\text{cm}^2$ for the thickness range of $0.3-1.0 \mu\text{m}$ accompanying the steep increase in the perpendicular lattice constant a_{\perp} . It is notable, however, that no streaky or cross-hatched surface morphology is found for these layers as mentioned above. If the value of the EPD of the grown layer increases a little more and reaches about $15 \times 10^3/\text{cm}^2$, the surface morphology of the specimens clearly indicates structural patterns. In this case, the thickness of the epilayers is larger than $\sim 2 \mu\text{m}$. These results suggest the existence of a threshold value of EPD. If the value of EPD exceeds this, the streaky or cross-hatched surface morphology is observed. From

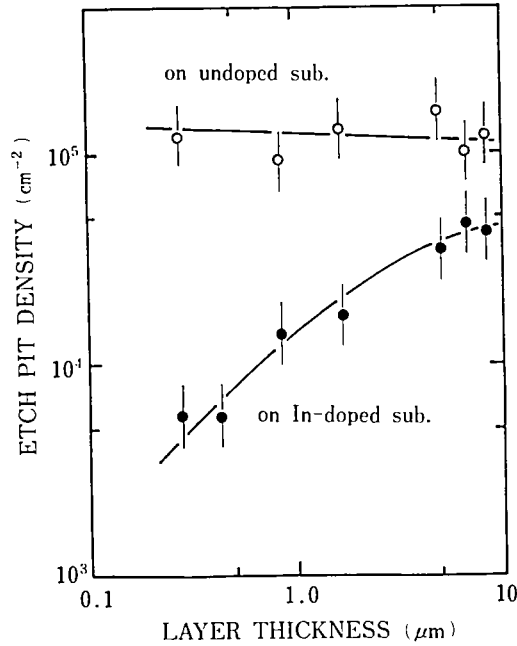


Fig. 9. Layer thickness dependence of the etch pit density observed at the surfaces of the epilayers grown at 600°C.²⁾

the results given by Fig. 7, for layers grown at 600°C and with thicknesses larger than $\sim 2\mu\text{m}$, the increase in the lattice constant a_{\perp} is not so steep and approaches that of undoped GaAs gradually. This tendency qualitatively coincides with the increase in the EPD for layers thicker than $\sim 2\mu\text{m}$. This means that the generation of misfit dislocations is almost completed if the layer thickness becomes larger than about $2\mu\text{m}$. The threshold value of the EPD will nearly correspond to the complete generation of cross-hatched dislocation arrays at the epilayer / substrate interface. After the propagation process from the interface to the surface, nearly complete generation of the dislocation arrays will bring about the structural pattern together with the threshold value of the EPD at the grown layer surface.

Concerning the above discussion, the value of the critical coherent length of our epilayer / substrate system is considered below. Indium atom content in the semi-insulating GaAs substrate used in this work is estimated from the value of the substrate lattice constant. The value of the lattice constant for $\text{In}_x\text{Ga}_{1-x}\text{As}$ varies linearly from that of GaAs, 5.6533 Å, to 6.0584 Å for InAs, according to the change of the x value from 0 to 1. As the value of the lattice constant measured for the In-doped substrate is 5.6585 Å, the deduced x value corresponds to an In atom content of $2.8 \times 10^{20}/\text{cm}^3$. The lattice mismatch f between the epilayer and the substrate [$\Delta a_{\perp}/a_{\text{sub}} = (a_{\text{film}} - a_{\text{sub}})/a_{\text{sub}}$] is also deduced from the values of a_{film} and a_{sub} . The evaluated value of f for the case of coherent growth is 9.2×10^{-4} in this work and the

calculated critical coherent length h_c of the epilayer is $0.17\mu\text{m}$ after both the formulas given by Matthews and co-workers⁸⁾ and those reported by Shinohara *et al.*⁶⁾ Thus, the obtained value of the coherent length, $h_c \doteq 0.17\mu\text{m}$, tentatively agrees with the results given by Figs. 7 and 9.

3.5. Photoluminescence study

Three kinds of specimens are studied by photoluminescence measurements at 4.2 K: (a) two specimens grown on an In-doped GaAs substrate at 500°C ; (b) two specimens grown on an In-doped GaAs substrate at 600°C ; and (c) a specimen grown on an undoped GaAs substrate at 600°C . The observed photoluminescence-peak wavelength, corresponding to the bound exciton peak, for the above five specimens is plotted against the layer thickness of the specimens as shown in Fig. 10.

The experimental data indicate the following: (1) The layer grown on an undoped substrate gives the exciton peak wavelength of about 819.3 nm (corresponding to the recombination energy or exciton energy of about 1.513 eV); (2) the layers grown on In-doped substrates have a longer wave-length than those of grown layers on undoped substrates; and (3) the layers grown at 600°C show a shorter wave-length than those for layers grown at 500°C .

The following explanation is applicable for the above results: (1) The measured value of the exciton peak wave-length of the layer grown on an undoped substrate coincides fairly well with the value of the bound exciton luminescence in pure GaAs;

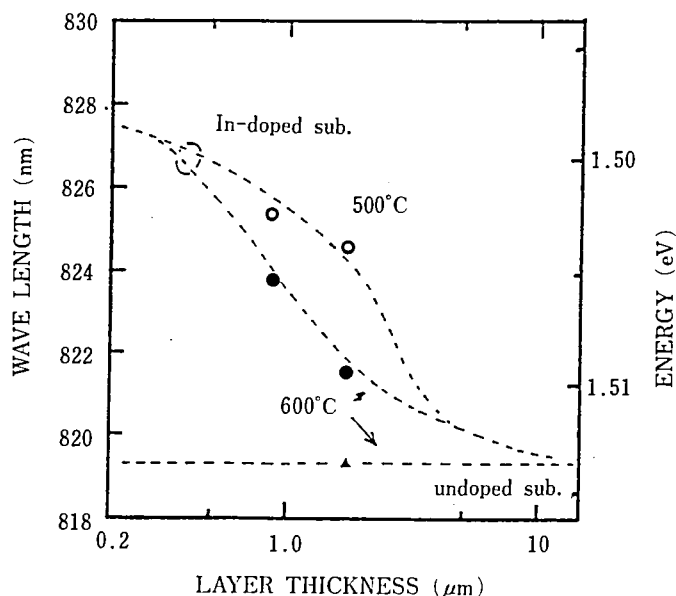


Fig. 10. Peak position of the exciton emission against the GaAs epilayer thickness for the specimens with various growth conditions.²⁾

(2)' the layers grown on In-doped GaAs have a smaller band gap than those of pure GaAs owing to the effect of strain or the two-dimensionally expanded stress originating from the lattice-mismatched heteroepitaxial growth; and (3)' the layers grown at higher temperature, 600°C, relieve the strain more rapidly than those grown at lower temperature, 500°C, indicating a steeper increase in band gap to approach the band-gap value inherent in pure GaAs.

Two dotted curves given in Fig. 10 are deduced semiempirically using the results given by Fig. 7 and also some assumptions. It is well known that the band gap E_g of GaAs increases monotonically by the application of hydrostatic pressure p according to $dE_g/dp = 9.4 \times 10^{-12}$ eV/dyn cm⁻². In the epilayers with coherently grown GaAs on heavily In-doped GaAs, the lattice constant a_{\perp} perpendicular to the (100) substrate plane obviously decreased as shown in Fig. 7. On the other hand, the lattice constant parallel to the (100) plane should increase two dimensionally in order to ensure the coherent epigrowth on the In-doped GaAs with larger lattice constant. Thus, in the epilayers grown on the In-doped substrate, expanded elastic strain will be included parallel with the substrate plane. This strain or bilateral tensile stress should cause a decrease in band gap.

The value of the longitudinal bilateral lattice constant a_{\parallel} of the coherently grown epilayers coincides with the lattice constant of In-doped GaAs substrate. With an increase in the epilayer thickness, the perpendicular lattice constant a_{\perp} begins to increase, accompanying the decrease in the bilateral lattice constant a_{\parallel} .

In the GaAs epilayers coherently grown on In-doped GaAs substrates, a volume of the elastically strained unit crystalline cell of the grown film is always larger than that of a pure or unstrained GaAs crystal cell. This stems from the fact that the bilaterally or two-dimensionally expanded strain $|\epsilon_{\parallel}| (= |(a_{\parallel} - a_0)/a_0|)$ is always larger than the perpendicular compressive strain $|\epsilon_{\perp}| (= |(a_{\perp} - a_0)/a_0|)$, where $a_0 = a_{\text{sub}}$ is the lattice constant of the GaAs substrate. The values of ϵ_{\perp} are directly obtained from the measured values of a_{\perp} and a_0 , while the values of ϵ_{\parallel} are indirectly calculated from the value of ϵ_{\perp} using the following equation: $\epsilon_{\parallel} = -(c_{11}/2c_{12})\epsilon_{\perp}$ where c_{11} and c_{12} represent the elastic stiffness constants for GaAs with the values of 1.188×10^{12} and 0.538×10^{12} dyn/cm², respectively. A negative sign in the above equation indicates that if ϵ_{\perp} is compressive, ϵ_{\parallel} is expanded. Then, if ϵ_{\perp} is compressive, the crystalline unit cell is in tension as a whole, because of the hydrostatic tensile component of the strain. The conversion from ϵ_{\perp} to ϵ_{\parallel} is necessary in order to know what kind of pressure, namely compressive or tensile pressure, is imposed on the unit cell of the coherently grown films. Thus, in order to know the relationship between the band gap or photoluminescence peak and measured a_{\perp} , a reasonable way is to convert the deduced ϵ_{\perp} to ϵ_{\parallel} . The opposite situations are reported for the $\text{Ga}_{1-x}\text{In}_x\text{P}$ epilayer/(100) GaAs system by Asai and Oe⁹⁾, indicating that the hydrostatic compressive component of the strain is imposed on the $\text{Ga}_{1-x}\text{In}_x\text{P}$ epilayer grown on GaAs.

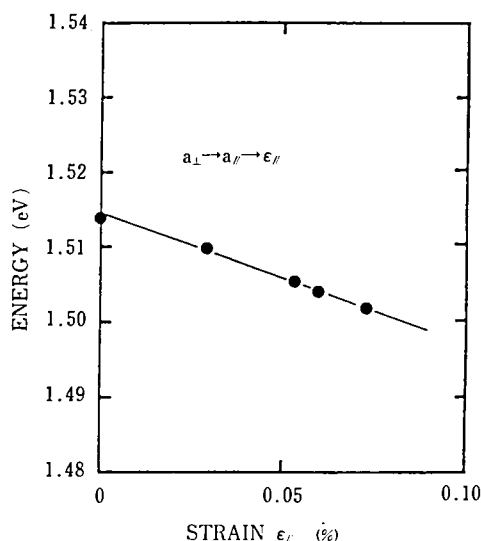


Fig. 11. Relationship between peak position of the exciton emission and the strain parallel to the surface of the epilayers grown on In-doped GaAs substrates. The experimental point at zero strain is obtained for the epilayer grown on a nondoped GaAs substrate.²⁾

By combining the photoluminescence data with the deduced $\epsilon_{||}$, the relation between exciton energy and $\epsilon_{||}$ is obtained as shown in Fig. 11. This shows that there is a linear relationship between them. As the layer thickness of the epilayer used in the above calculation is known, the experimental curves given by Fig. 7 are transformed to curves showing the relation between the layer thickness and exciton energy or photoluminescence-peak wavelength and thus the two dotted curves shown in Fig. 10 are obtained. The curves reflect the relaxation process from the coherently grown lattice to that inherent in pure GaAs. The dependence of epigrowth temperature on the relaxation process is also obvious.

3.6 Thermal annealing effects

The thermal annealing effects on both the surface morphology and the lattice constant a_{\perp} of epilayers are examined. Two specimens are annealed on the susceptor after the epitaxial growth in the AsH_3 gas flow to prevent the evaporation of As. The annealing temperature is held at 600°C for the epilayer grown at 500°C , while at 700°C for the one grown at 600°C .

The surface morphology of these specimens before and after the annealing is illustrated in Figs. 12 and 13. Figure 12 (a) shows the surface morphology for the epilayer grown at 500°C for 1 h and before the annealing. This indicates a clear, mirror-like smoothness. Figure 12 (b) shows the surface pattern observed for the

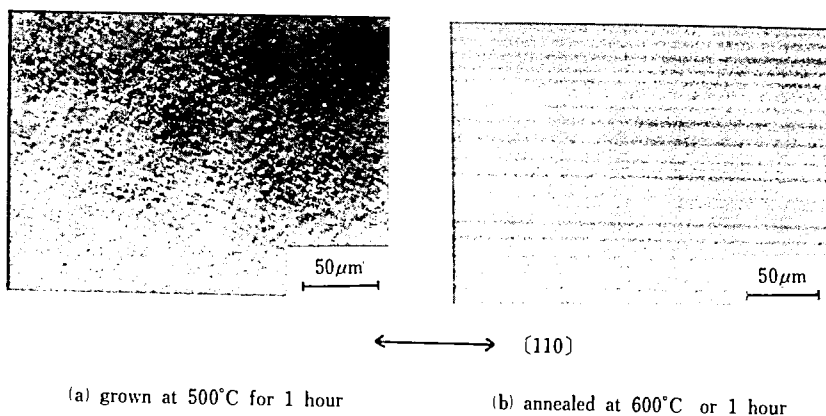


Fig. 12. Surface morphologies of (a) an asgrown GaAs epilayer on an In-doped GaAs substrate grown at 500°C for 1 h and (b) the same specimen annealed at 600°C for 1 h.³⁾

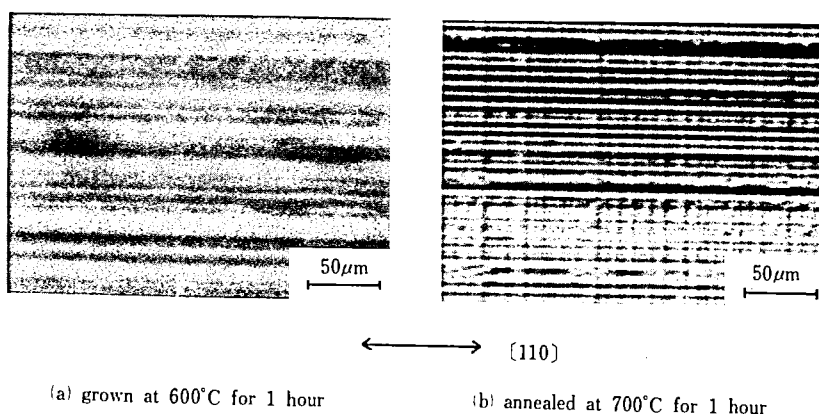


Fig. 13. Surface morphologies of (a) an asgrown GaAs epilayer on an In-doped GaAs substrate grown at 600°C for 1 h and (b) the same specimen annealed at 700°C for 1 h.³⁾

same specimen after 1 h thermal annealing at 600°C. This indicates quite different surface morphology from that in Fig. 12 (a) and a clear streaky (or weakly cross-hatched) structure is observed.

Figure 13 (a) shows the surface morphology for the epilayer grown at 600°C for 1 h and before the annealing. In this case, a streaky structure pattern has already appeared. Figure 13 (b) is the surface pattern observed for the same specimen with Fig. 13 (a) besides the thermal annealing for 1 h at 700°C. This shows not only the appearance of a streaky pattern with closer spacing but also a cross-hatched pattern. Narrowing of the streaky line spacing implies a larger quantity of dislocation generations through the epilayers. The appearance of the cross-hatched pattern

reveals the enhancement of the $[1\bar{1}0]$ direction dislocation array generation.

The perpendicular lattice constant a_{\perp} of these specimens is also found to change during the thermal annealing process. Figure 14 shows the relationship between the epilayer thickness versus the lattice constant a_{\perp} for the two series of specimens. One is epi grown at 500°C and the other at 600°C. Both are grown on heavily In-doped GaAs²⁾. The obtained changes in the lattice constant a_{\perp} by thermal annealing are shown by two arrows at the given film thickness.

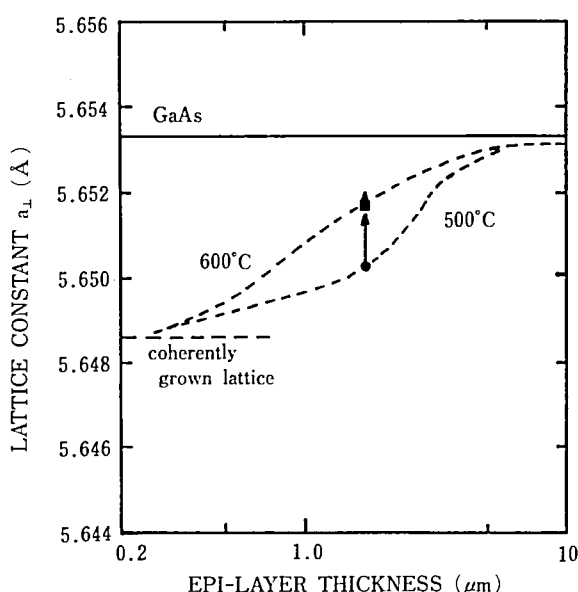


Fig. 14. Relationship between the epilayer thickness and the perpendicular lattice constant a_{\perp} of the epilayer grown at 500 and 600°C. Two arrows show the changes in a_{\perp} caused by the thermal annealing process.³⁾

It can be suggested from these results that the lattice constant a_{\perp} is primarily determined by the film thickness especially found for those grown at 600°C. As the epilayer thickness becomes larger, the lattice constant a_{\perp} also becomes larger, implying the larger extent of relaxation from the coherently grown lattice to that which is inherent in pure GaAs.

For the epilayer grown at 500°C, the thermal annealing process brings about an appreciable increase in the lattice constant a_{\perp} . Through this process, the generation of mismatch dislocation arrays is enhanced and streaky surface morphology together with an appreciable increase in a_{\perp} is shown. This increase in a_{\perp} , however, is finally limited by the value of a_{\perp} primarily determined by the epilayer thickness.

3.7 Zinc doping effects

A study to obtain coherently grown GaAs epilayers as thick as several μm on In-doped GaAs substrates is also underway. If such epilayers are obtained, essentially no dislocations will be included in the layers. A dislocation-free GaAs epilayer on an In-doped GaAs has been obtained by In doping using the MBE technique⁷⁾.

In our study, Zn atoms are doped (order of $3 \times 10^{20}/\text{cm}^3$) during the OM-VPE process at 500°C of growth temperature. The unstrained Zn-doped GaAs epilayer can be grown on the undoped GaAs substrate and the lattice constant of the Zn-doped GaAs is the same as that of the undoped GaAs. Figure 15 shows the relation between the Zn-doped epilayer thickness and the lattice constant a_\perp evaluated from x-ray diffraction analyses. The results shown in Fig. 15 indicate that the epilayers with nearly the same value as that of the coherently grown lattice, $a_{\perp c} = 5.6486 \text{ \AA}$, are obtained even for epilayers as thick as several μm . The dotted line given in Fig. 15 shows the relation obtained between the as-grown GaAs epilayer thickness and the lattice constant a_\perp .

In the case of non-Zn-doped epilayers, a_\perp increases with an increase in epilayer thickness and finally approaches the value inherent in pure GaAs. It is clear that this

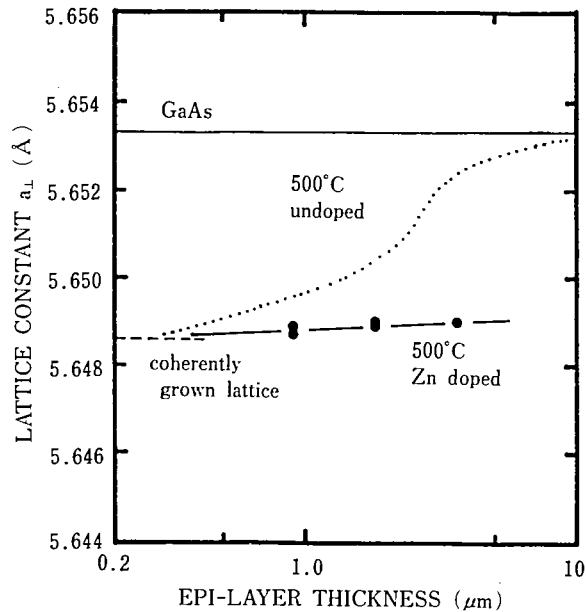


Fig. 15. Relationship between the Zn-doped (order of $3 \times 10^{20}/\text{cm}^3$) epilayer thickness and the lattice constant perpendicular to the substrate surface, a_\perp , for the growth on the In-doped GaAs substrate at 500°C . The dotted line is the relation between the lattice constant a_\perp and the epilayer thickness grown at 500°C . The broken line indicates the coherently grown lattice, $a_\perp = 5.6486 \text{ \AA}$, of the epilayer on the In-doped substrate.³⁾

increase in a_{\perp} reflects the generation of misfit dislocation arrays through the epilayers. Therefore, epilayers with a lattice constant value close to that of pure GaAs indicate a structural or streaky surface morphology as shown in Fig. 12 (b). The measured etch pit density (EPD) at the surface of various epilayers is given in Fig. 16. As speculated above, a large quantity of EPD (more than $10^3/\text{cm}^2$) is observed even for epilayers grown at 500°C if Zn doping has not been accompanied. In this case, if the layer thickness becomes lower than about $0.5\mu\text{m}$, the value of EPD becomes unmeasurably small corresponding to the relation obtained between the lattice constant and the grown epilayer thickness shown in Fig. 15. For the Zn-doped epilayers grown at 500°C , no appreciable EPD is found to be consistent with the coherent growth of the layers. When an unstrained undoped GaAs layer is grown on an undoped LEC crystal having threading dislocations of the order of $10^5/\text{cm}^2$, the same order of high density dislocations appears at the epilayer surface which is

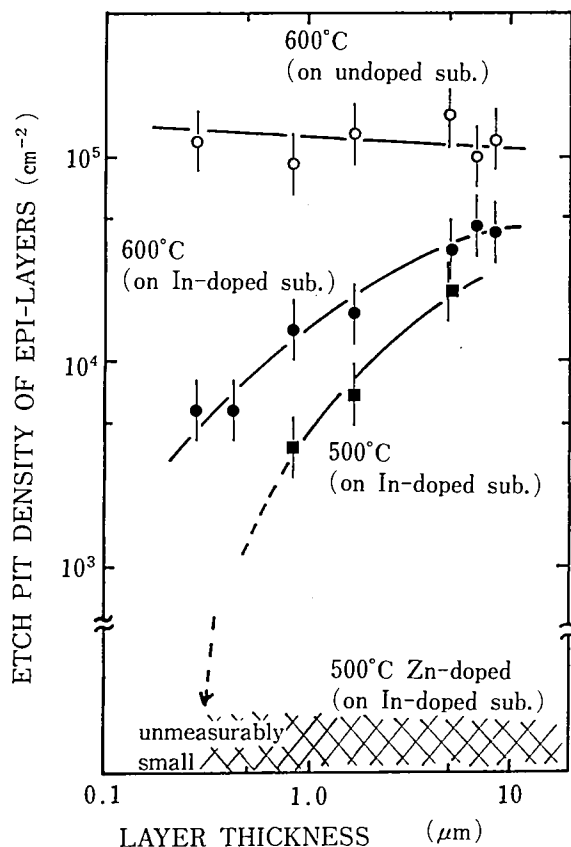


Fig. 16. Relationship between the etch pit density (EPD) at the surface of various epilayers and the epilayer thickness. No appreciable EPD is found for the Zn-doped epilayers grown at 500°C .³⁾

verified by EPD observation.

Recently, Deppe *et al*¹⁰⁾ reported in their paper that low-temperature Zn diffusion (600°C) is effective in reducing the dislocation density in GaAs epilayers grown on Si by MBE. And the reduction in the dislocation density that occurs with Zn diffusion is suggested to be due to the increased concentration of point defects generated during the Zn diffusion, resulting in an enhanced dislocation climb. Their paper reports the reduction of dislocation already generated before the Zn diffusion; however, our present work shows almost no generation of dislocations by Zn doping during the epitaxial growth. Although the possibility of the similar suggested mechanism with that of Deppe's paper may be taken into account, the present Zn doping effects on the lattice constant a_{\perp} are likely to be based on a different mechanism, such as impurity hardening. More precise investigation to clarify the Zn doping effect in this work is needed.

4. CONCLUSIONS

OM-VPE grown GaAs layers on heavily In-doped GaAs substrates are investigated in some detail. It is found that some correlations exist not only between the surface morphology and the perpendicular lattice constant a_{\perp} , but also between the surface morphology and the grown layer thickness. These correlations are explained by the relaxation process from the coherently grown epilayer lattice to that inherent in pure GaAs. The correlations also depend on the temperature at the epigrowth, as might be expected.

Epilayers on In-doped GaAs have a coherently grown lattice at a thin enough layer thickness. As the epilayer thickness increases, the generation of misfit dislocation arrays along $\langle 110 \rangle$ directions occurs at the epilayer/substrate interface. These dislocation arrays propagate towards the epilayer surface and are observed as streaky or cross-hatched lines together with an appreciable increase in perpendicular lattice constant a_{\perp} . If the generated dislocations are smaller than some definite value, the surface morphology of epilayers is mirrorlike corresponding to a significantly smaller increase in the value of a_{\perp} .

Our photoluminescence study also confirms the relaxation process mentioned above. Namely, as the epilayer thickness increases, exciton peak energy increases, implying the decrease in two-dimensionally expanded stress along (100) planes of the substrates. The dependence of epigrowth temperature on the relaxation process is also apparent from the difference of the observed values of exciton energy for the specimens grown at different temperatures.

The dislocation arrays that appear at the layer surface are found to be enhanced by the annealing process after GaAs epilayer growth on the In-doped GaAs substrate. The changes in the perpendicular lattice constant a_{\perp} as well as changes in the surface morphology of epilayers are observed. It is also found that Zn doping is very effective to obtain thick, coherently grown GaAs epilayers on In-doped GaAs

substrates. No appreciable changes in a_{\perp} or generation of misfit dislocations are found because of the hardening of the crystalline lattice. The Zn atom will therefore play an important role as that of In in the case of dislocation-free In-doped LEC crystal growth.

ACKNOWLEDGMENTS

The author wishes to express his sincere thanks to Dr. S. Fuke, Mr. K. Mori, and also to Mr. Kuwahara at Shizuoka University.

Mr. K. Mori now belongs to Seiko Epson Co. and this work has been done as his Bachelor and Master theses studies under the guidance of the author and Dr. S. Fuke.

Thanks are also due to the ULVAC Co. for providing the OM-VPE apparatus.

REFERENCES

- 1) T. Imai, S. Fuke, K. Mori, and K. Kuwahara : Growth of GaAs epitaxial layers prepared in the laboratory with an integrated safety MOCVD system, *Appl. Surf. Sci.* **33/34**, pp. 587-593 (1988).
- 2) T. Imai, S. Fuke, K. Mori, and K. Kuwahara : Some properties of organometallic vapor-phase epitaxial grown GaAs layers on In-doped GaAs substrates, *J. Appl. Phys.* **65**, pp. 3877-3882 (1989).
- 3) T. Imai, S. Fuke, K. Mori, and K. Kuwahara : Thermal annealing and zinc doping effects on the lattice constant of organometallic vapor phase grown GaAs epilayers on heavily In-doped substrates, *Appl. Phys. Lett.* **54**, pp. 816-818 (1989).
- 4) M. Morioka, T. Mishima, K. Hiruma, Y. Katayama, and Y. Shiraki, in *Proceedings of International Symposium on GaAs and Related Compounds*, Karuizawa, Japan, 1986 (Institute of Physics, London, England), p. 121.
- 5) M. Shinohara, T. Ito, and Y. Imamura, *J. Appl. Phys.* **58**, p. 3449 (1985).
- 6) M. Shinohara, T. Ito, K. Yamada, and Y. Imamura, *Jpn. J. Appl. Phys.* **24**, L711 (1985).
- 7) H. Takeuchi, M. Shinohara, and K. Oe, *Jpn. J. Appl. Phys.* **25**, L303 (1986).
- 8) W. Matthews, A. E. Blakeslee, and S. Mader, *Thin Solid Films*, **33**, p. 253 (1976).
- 9) H. Asai and K. Oe, *J. Appl. Phys.* **54**, p. 2052 (1983).
- 10) D. G. Deppe, N. Holonyak, Jr., K. C. Hsieh, D. W. Nam, W. E. Plano, R. J. Matyi, and H. Shichijo, *Appl. Phys. Lett.* **52**, p. 1812 (1988).